

## GEOPHYSICAL SIGNATURE OF THE VIEN-TYPE URANIUM MINERALIZATION OF WADI EISHIMBAI, SOUTHERN EASTERN DESERT, EGYPT

I.M. Gaafar

Nuclear Materials Authority, Cairo, Egypt, Email: gaafar\_ibrahim@yahoo.com.

البصرة الجيوفيزيائية لتمعدنات اليورانيوم العرقى بوادى إسيمباى، جنوب الصحراء الشرقية، مصر

**الخلاصة:** تهتم هذه الدراسة بتمعدنات اليورانيوم في وادى إسيمباى، جنوب الصحراء الشرقية جنوبية بمصر. تعرضت منطقة الدراسة للعديد من القواطع التى غالبا ما تأخذ الاتجاهات شرق شمال الشرق. غرب جنوب الغرب. تتكون هذه القواطع من بللورات كبيرة من الفلسبارات البوتاسية منغرسية فى أرضية ذات بللورات قاعدية دقيقة غنية بالكالسيت تسمى "لامبروفير". تسببت قوى الضغط الشديدة فى الإتجاه شمال الشرق. جنوب الغرب الى الفتح فى نفس الإتجاه نتيجة لقوى الشد فى الإتجاه العمودى (شمال شمال الغرب. جنوب جنوب الشرق). توجد بعض ظواهر التغيرات الشديدة نتيجة تأثير سلسلة متوازية من الفوالق التى تضرب فى الإتجاه شمال شمال الغرب. جنوب جنوب الشرق مسببة إزاحة أفقية يسارية. ونتيجة لإعادة نشاط نفس الحركات التكتونية فقد ظهر العديد من عمليات التغيرات على نطاقات القص التى غالبا ما ترتبط بزيادة وإعادة تركيز تمعدنات اليورانيوم. لذلك فإن تلك العمليات التكتونية المعقدة تمثل ظواهر هامة لخصوبة المنطقة لاحتواء خام اليورانيوم.

لتحقيق البصرة الجيوفيزيائية لتمعدنات اليورانيوم المرتبطة بالمنطقة تم تطبيق طرق الإشعاع الطيفى الجامى، الكهرومغناطيسية منخفضة التردد والمغناطيسية. ومن خلال التفسير المتكامل لخرائط الإشعاع الطيفى الجامى، وجد أن نطاق القص قد تميز بالزيادة الشديدة فى محتواه من اليورانيوم وانخفاض كل من البوتاسيوم والثوريوم. وقد تراوحت قيم اليورانيوم المكافئ من 20 ppm إلى 140 ppm فى نطاق القص الممتد فى الإتجاه شمال-جنوب. وتتميز اللامبروفير بشاذات يورانيوم عالية تزيد عن 90 ppm وتمتد فى الإتجاه شرق - غرب. بينما ترتبط أعلى قيمة لشاذات اليورانيوم (700 ppm) بالجرانيت المتغاير بالجزء الغربى من المنطقة والممتد فى اتجاه شمال-جنوب. أوضحت طريقة الكهرومغناطيسية منخفضة التردد وجود نطاقات ضحلة ذات قدرة توصيلية عالية، وهى الظواهر الأبرز على الخرائط الخاصة بتلك الطريقة. أعطت طريقة المغناطيسية صورة واضحة عن الوضع التحتسطحي ومبينة أن عروق اللامبروفير لها جذور ممتدة فى العمق. ومن تكامل نتائج الطرق الجيوفيزيائية، أمكن تحديد نطاق القص بدرجة تفصيل عالية جدا وأنه ممتد لأكثر من 600 م تحت السطح ومنفصل بمسافات بينية نتيجة للفوالق الممتدة فى اتجاه شمال شمال الغرب-جنوب جنوب الشرق والتى أدت إلى إزاحة يسارية جانبية.

**ABSTRACT:** The application of various geophysical tools with different responses succeeded in fixing U-mineralization in Wadi Eishimbai area. The area was studied using detailed ground spectrometric, magnetic and VLF-EM surveys.

The interpretation of the obtained spectrometric maps clearly reflects the sharp increase of eU content. Meanwhile, the K- and Th-contents show sharp decreases. The eU/Th ratio correlates positively with eU concentrations and negatively with eTh concentrations, indicating an increase in the U-potentiality than the surrounding granite. The N-S shear zone displays an eU content ranging from 20 to 140 ppm. The ENE- trending lamprophyre is characterized by elongated uranium anomalies trending in the E-W direction, with values >90 ppm. Equivalent uranium content of the brecciated granite attains values up to 700 ppm.

The ground magnetic and VLF-EM surveys played important roles in providing structural information, which proved useful in geological mapping and mineral exploration for the discovery of the uranium mineralization in the study area. This study follows the expected subsurface extension of the Sela shear zone, under Wadi sediments. The ground total magnetic-intensity map shows a relatively narrow and an elongated shape for the lamprophyre anomaly which extends for about 600m in the Wadi towards the west direction.

The filtered very low frequency electromagnetic (VLF-EM) contour maps of the two used frequencies (17.1 and 28.5 kHz) show an excellent agreement, indicating that the shear zone is distinguished with somewhat or relatively strong conductivity westwards, as an extension for the main shear zone. It is elongated in an ENE-WSW trend, and extends in the western direction, referring to the existence of conductive materials.

Most of the NW-SE trending faults cause sudden changes in the magnetic and VLF-EM contour spacing over an appreciable distance, which suggests a discontinuity in depth due to their left-lateral strike-slip displacements. The interpreted faults, with an ENE-WSW trend represent the main trend of Sela shear zone, through which hydrothermal solutions flowed causing high alteration and uranium mineralization.

### 1- INTRODUCTION

Wadi Eishimbai area is located in the Southern Eastern Desert of Egypt, between Latitudes of 22° 17' 12" N - 22° 18' 7" N and Longitudes of 36° 12' 54" E

and 36° 13' 50" E, at a distance of about 35 km to the southwest of Abu-Ramaad city (Fig. 1). The influence of the ENE-WSW structural trend (the main shear zone in Sela granite) in the successive structural events make

its evolutionary history a good guide to describe the lithologic and structural history of Wadi Eishimbai area.

The integration of some geophysical methods, such as electrical resistivity, electromagnetic and magnetic as lithological and structural mapping tools were confirmed by several authors (e.g., Kowalik and Glenn, 1987; Barker et al., 1992). Large areas of the world were covered by ground and airborne gamma-ray surveys and many national and regional radiometric maps were compiled and published (IAEA, 2003). Several occurrences of strongly-altered ultramafic units were located on the basis of correlation between aeromagnetic signatures and airborne radiometric results, and one of them directed to further exploration and located a mineralized zone (Airo, 2007).

An interpreter experienced in magnetic can usually see structures nearly by looking at a magnetic map, much as one can visualize surface features from the contours of a topographic map (Telford et al., 1990). In this study, it is intended through geological and magnetic mapping, to obtain the optimum conditions for detecting the uranium-mineralization material in a highly-magnetized sheared lamprophyre in the study area. The exploration in the Wadi Eishimbai area was directed to define the subsurface structural pattern for a vein type of uranium mineralization with strong contrasts in magnetic susceptibility. Besides, the deep nature of the magnetic data provides direct exploration vectors for determining the optimum drilling locations for the expected subsurface uranium ore deposit.

VLF radio transmitters, operating in the 15–30 kHz frequency bandwidth provide an electromagnetic source for geophysical investigation. The VLF method proved to be an effective exploration tool for massive sulphides, graphites, carbonaceous shales, sheared contacts, and fracture zones. Therefore, during the last decades, it was employed world-wide to identify conducting features in mineral exploration, geological, engineering and environmental problems (Barbour and Thurlow, 1982; Fischer et al., 1983; Sinha and Hayles, 1988; McNeill and Labson, 1991; Chouteau et al., 1996; Gharibi and Pedersen, 1999; Oskooi and Pedersen, 2001; Becken and Pedersen, 2003). The principle of VLF surveying was described by Spies (1989), Vallee et al. (1992), and Kaikkonen and Sharma (2001). In this study, the strong contrasts in electrical conductivity provided direct exploration vectors for the uranium-mineralized materials through the use of VLF- EM.

## 2. GEOLOGY

The granite pluton which is located to the east of the investigated area was subjected to detailed studies comprising field geological and geophysical mapping by Gaafar (2005). The ENE-WSW lamprophyre dykes dissecting the north granites are massive, fine-grained black groundmass, with alkali feldspar phenocrysts. They have higher U-content, many times greater than

the granite. Many promising criteria to find uranium ore were reached, especially those related to the ENE-WSW shear zone. Many generations of silica as well as microgranite and lamprophyre dykes enriched in uranium were recorded. Polyphases of alteration processes, superimposed the emplacement of these injections, are structurally-controlled and well defined through the ENE-WSW shear zones and the nearly perpendicular N-S fault set (Fig. 1). These zones were the channel for the fluids, involved in all the uranium concentration steps, which may lead to the formation of U-ore bodies in the area.

The importance of lamprophyre in remobilizing and concentrating the uranium minerals make it useful to compile the expected subsurface extensions of this rock. According to the strong contrast between the magnetic susceptibilities of the sheared basic lamprophyre, and the surrounding granites, magnetic survey is necessary for determining the expected subsurface extension of the shear zone and its contacts with the surrounding rocks. This is very important for determining and recommending the locations, dips and depths of drilling.

The detailed geological field work distinguished two main granitic phases in the central part of the studied area. The earlier one is the coarse-grained biotite granite, which is located to the east. The second one is the medium-grained two-mica granite, which is exposed in the western part of the pluton as patches which crosscut the coarse granite (Fig. 1). The brecciated granite in this area is leucocratic and mainly composed of quartz, feldspars and muscovite/biotite mica. Some intensive alteration features, such as hematization and illitization are recorded where a set of parallel N-S faults are present. This granite is highly weathered and its bulk volume disappeared and representing low land granitic masses. Meanwhile, the more resistive jasper and white silica represent the highest peaks. The process of uranium mobilization is very important as such altered rocks were subjected to mineralized bearing solutions.

## 3. GROUND GAMMA-RAY SPECTROMETRIC SURVEY

Several recent studies have shown the usefulness of gamma-ray spectrometric surveys for abandoned mine site characterization (e.g., Winkelmann et al., 2001; Martin et al., 2006).

Ground spectrometric measurements were conducted to cover a variety of lithologies and various degrees of alterations associated with the uranium mineralization in the study area. The lamprophyre is characterized by abnormally high eU content (Gaafar et al., 2006).

One field characteristic of the mineralized brecciated granite is pervasive alteration and higher degree of fractionation than normal fresh granite. The

radon concentrations are aligned along the NNW direction, forming many anomalies with different amplitudes and different magnitudes ranging between 18000 and 190300 Bq.m<sup>-3</sup> (Gaafar et al., 2010). This enrichment in uranium on the expense of both thorium and potassium is associated with the occurrence of discrete uranium minerals.

### 3.1. Field Procedure and Measuring Equipment

Ground radioelement concentration measurements were carried out over the studied area in the form of a uniform grid (40 m × 20 m interval), with dense grid spacing (5 m interval) over the high by mineralized parts. The measurements were conducted using a Czech-made Geophisica Brno GS-256 spectrometer, having a 0.35l sodium iodide (NaI) thallium (Tl) activated detector. The spectrometer is well calibrated on artificial concrete pads, containing known concentrations of K, U and Th. The radiation energy spectrum depicts the relative count rates in the range between 0.12 and 3.0 MeV. U, Th and K were determined by analyzing the  $\gamma$ -radiations from <sup>238</sup>U, <sup>232</sup>Th and <sup>40</sup>K, recorded at different windows (Chiozzi et al., 2000). For the determination of eU and eTh, the selected peaks and energy values were <sup>214</sup>Pb at 1.76 MeV and <sup>208</sup>Tl at 2.62 MeV, respectively. Potassium was directly determined from the window centered at 1.46 MeV corresponding to the primary decay of <sup>40</sup>K.

### 3.2. Gamma-Ray Spectrometric Results

Studies on the concentration and the distribution of the three naturally-occurring radioelements are of considerable interest in geophysics. They are useful in theoretical applications, such as modelling the underground thermal structure, because U, Th and K are the main sources of radiogenic heat in the rocks (Chiozzi et al., 2002). In the present study, the  $\gamma$ -ray spectrometric contour and ratio maps (K, eU, eTh and eU/eTh) for the study area were prepared and subjected to detailed interpretations.

#### 3.2.1. Potassium (K %) contour map

The potassium surface distribution contour map (Fig. 2) shows that the lowest potassium contour line values (<1.0 %) are associated mainly with Wadi sediments. The ENE-trending lamprophyre and the N-S trending brecciated granite are well discriminated with their elongated shapes and low K levels. The Wadis around the granites are contoured with potassium concentrations ranging from 1.0 to 2.4 %. The two-mica granite shows potassium content, ranging from 3.5 to 5.0 %. It is encountered as zones of irregular shapes that are mainly elongated in the two main structural trends in the area (NNW-SSE and ENE-WSW). This increase in K content results from the highly-fractured granite beside the intrusions of late-magmatic fine-grained granite, which are characterized by their high radioactivity levels.

#### 3.2.2. Equivalent uranium (eU, ppm) contour map

The N-S trending shear zone, the ENE-trending lamprophyre and the brecciated granite are all characterized by strong eU concentration anomalies (Fig. 3).

The contour lines with values, less than 2 ppmeU are observed over Wadi sediments around the granite. The eU range (2-10 ppm) is shown over the medium-grained two-mica granite. It is encountered as zones with different shapes, sometimes controlled by the main fault trends in the study area. The N-S shear zone displays an eU content ranging from 20 to 140 ppmeU. It shows sharp gradients with the two-mica granite. Such high range or level is encountered as elongated domains trending in the NNW-direction along the main faults. These eU anomalies reflect secondary uranium remobilization along these fault zones.

The ENE- trending lamprophyre which crosses the northern part of two-mica granite, plays an essential role in the uranium remobilization processes. It is characterized by elongated anomalies trending in the E-W direction, with values >90 ppmeU. These altered rocks were subjected to mineralization-bearing solutions, where the shear zone acts as a good trap for U-rich fluids.

Equivalent uranium content of the brecciated granite attains values up to 700 ppmeU with relatively low eTh and K contents. Such locations proved to possess high U-potentialities in the study area. This high U-potentiality is typically associated with the alteration of the sheared rocks, which are associated with uranium mineralization. This is best developed along the western part of the study area.

#### 3.2.3. Equivalent thorium (eTh, ppm) contour map

Thorium content usually reflects the original rock varieties and the fractionation in this type of granites, when thorium content increases. Therefore, eTh content contour map (Fig. 4) shows well discrimination between the western two-mica granite and the eastern biotite granite. The eastern parts of biotite granites have moderate values, ranging from 8 to 30 ppm. In contrast, the eTh content of the two-mica granite in the western part of the studied area is characterized by a wide range oscillating from 10 to > 80 ppm eTh, having different shapes of anomalies that are affected by the structural setting of the study area. Most of the shear zone is occupied by eTh-anomalies. These anomalies have oval-shapes and trend nearly in the NNW direction.

The eTh contours along Wadi sediments have values ranging from less than 0.2 to 5 ppm. They define zones with different shapes, distributed all over the whole Wadi sediments.

The western part of the area of lowland and the highly-weathered brecciated granite are characterized by eTh contour lines with moderate values, ranging from 7 to 35 ppm.

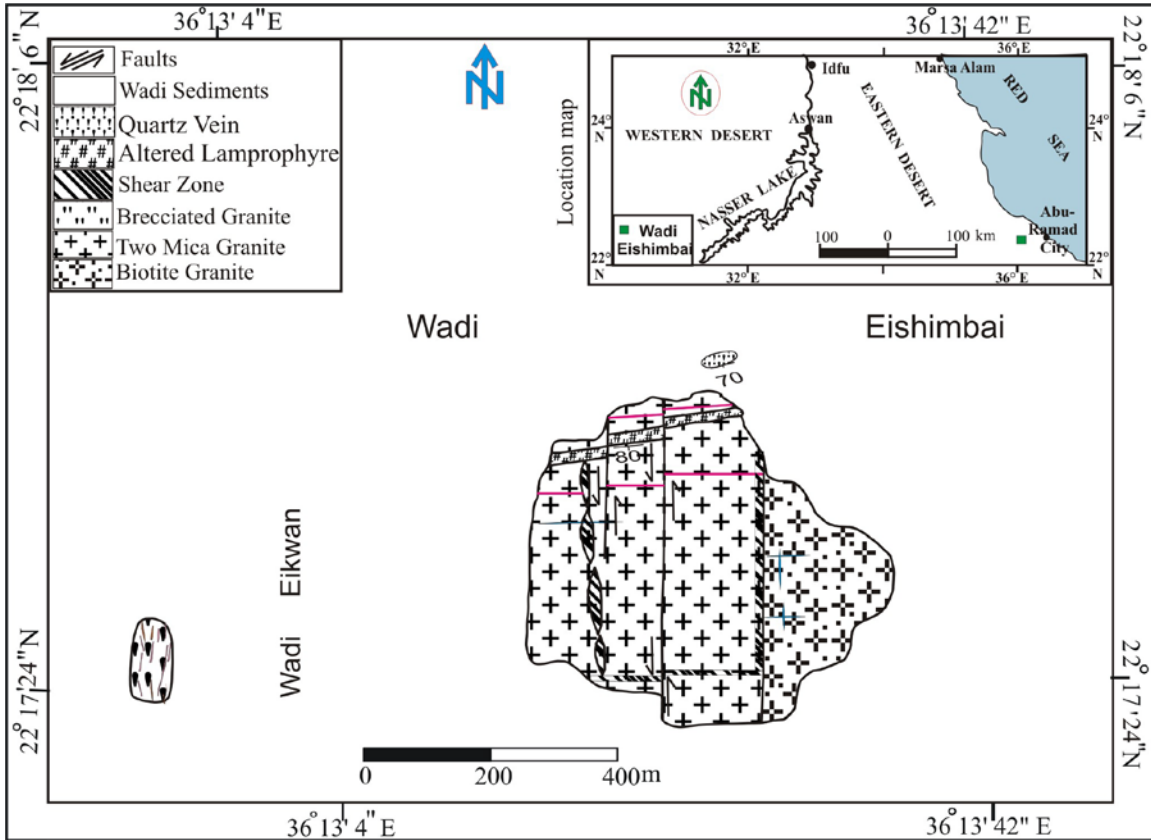


Fig. (1): Geologic and location map of Wadi Eishimbai area, Southern Eastern Desert, Egypt.

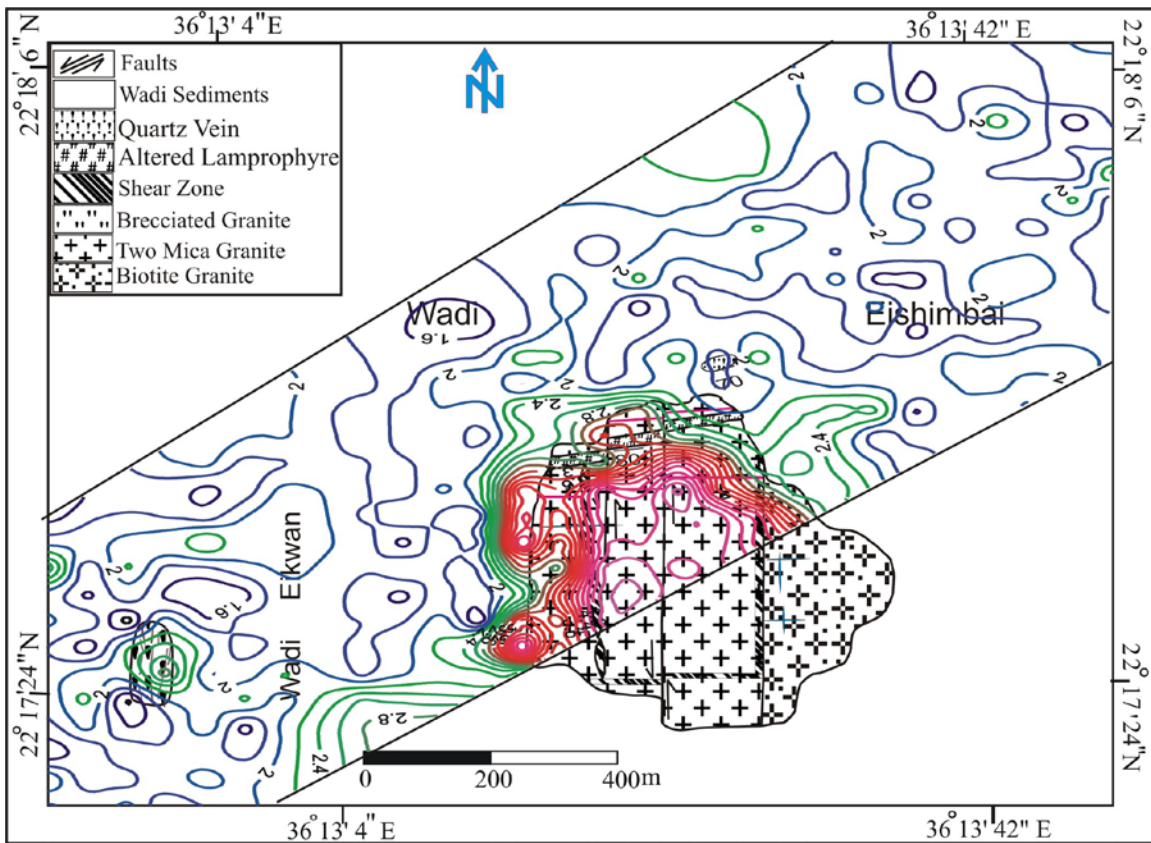


Fig. (2): Potassium (K, %) contour map of Wadi Eishimbai, Southern Eastern Desert, Egypt.

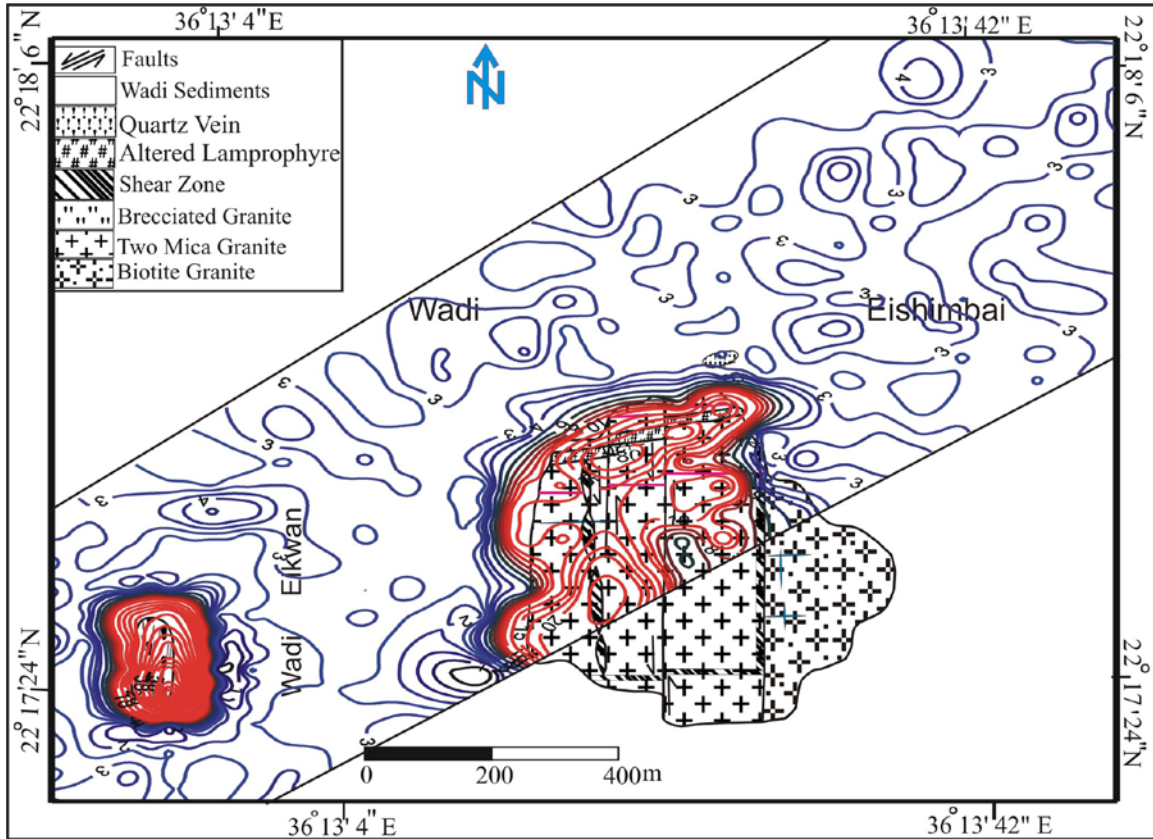


Fig. (3): eU (ppm) contour map of Wadi Eishimbai area, Southern Eastern Desert, Egypt.

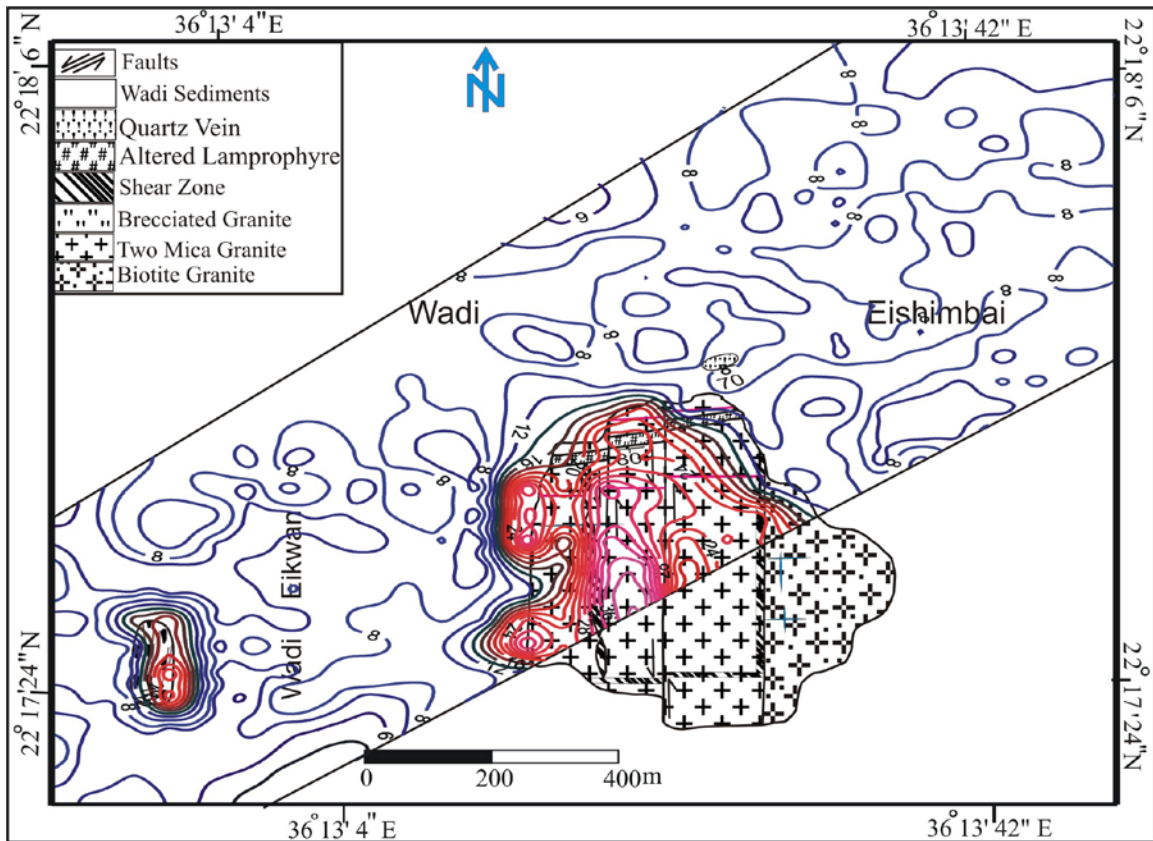


Fig. (4): eTh (ppm) contour map of Wadi Eishimbai area, Southern Eastern Desert, Egypt.



The unaltered lamprophyre occurring in the northern part of the two-mica granite possesses elongated low values, reaching 20 ppm eTh.

#### 3.2.4.- eU/eTh ratio contour map

The general view of the surface eU/eTh ratio distribution map of the study area (Fig. 5) indicates that the brecciated granite shows promising anomalies and their radiometric signatures are characterized by dense contours, elongated in the N-S direction in southwestern part of the study area. However, eU/eTh ratio contour map clearly exhibits distinctive anomalies over the lamprophyre. These strong anomalies show raised amplitudes, resulting in obvious exploration targets. This is demonstrated particularly well in the form of a high concentric anomaly, elongated in the ENE-direction, and located in the northern part of the two-mica granite. Meanwhile, the N-S shear zone shows also high content of eU over eTh levels, trending in the NNW-direction. A fractured controlled U-mineralization is located within the shear zone in the granite, in the western part of the biotite granite. This vein type mineralization possess higher U-content many times greater than the granite, leading to an increase in the U-potentiality, which might led to U-mobilization and possibly local uranium entrapment in the study area.

## 4. GROUND MAGNETIC SURVEY

One of the most useful geological applications of magnetic surveys is to map structural trends by following lineations of magnetic contours (Dobrin and Savit, 1988). The magnetic anomalies are frequently related to fractures, either through the control of deposition or the emplacement of magnetic materials by preexisting fracture system or by the dislocation of boundaries between formations of different magnetizations.

The main aim of any magnetic study is to recognize the depth, position, shape and attitude of the responsible magnetic bodies, and then interpret these parameters in terms of geological models which are consistent both with the observed geology and the accepted postulated geological models (Boyed, 1969). The exploration in the study area was directed to define the subsurface structural pattern for the uranium mineralization with contrasts in magnetic susceptibility. Besides, the deep penetration of the magnetic data provides direct exploration vectors for determining the optimum drilling locations for the expected subsurface uranium ore deposit.

### 4.1. Field Procedure and Measuring Equipment

The present survey includes the area to the west of the shear zone attaining one kilometer in length and with a width of 400 m, using a uniform square grid of (40×40 m). All the ground magnetic measurements were collected using the Scintrex proton magnetometer and the VLF-EM; Canada-model ENVI.

## 4.2. Magnetic Results and Interpretation

### 4.2.1. Total Magnetic Field Intensity Map

The total magnetic field intensity map (Fig. 6) contains many nearly-circular positive and negative anomalies located to the northeast and extend over Wadi sediments to about 300 m, without any surficial outcrops' exposed of the shear zone. This indicates the continuity of the shear zone in the subsurface that is responsible for these magnetic anomalies. The shear zone is exposed again to the southwest far away from the main shear zone by about 600m. It extends to about 300 m and trends in the ENE-direction. It is mostly lamprophyre, without silica vein. It is characterized by high eU content, reaching to more than 130 ppmeU without any increase in eTh content. This indicates that the uranium enrichment is post-magmatic due to the remobilization of uranium from the adjacent granite and its reconcentration in the sheared lamprophyre. Comparing the contour map with its geologic background (Fig. 6), it is evidence that the magnetic anomaly has broad limits than the exposed lamprophyre, which refers to its broad root.

The northern contact between the granitic body and the Wadi sediments is characterized by an elongated and low-amplitude magnetic signature, trending in the ENE-WSW direction, parallel to the main shear zone. It is bounded by the contour line 240 nT and extends continuously over Wadi sediments with a linear shape to the southwest for about 1.0 km. This well-defined boundary between these zones, with appreciably low degrees of magnetic relief, can indicate the presence of a major basement fault. It is mostly associated with the thrust contact between the granite and basic rocks to the north. Generally, the total magnetic intensity values increase towards the northern part of the studied area. This is due to the presence of basic country rocks, which have broad extension underneath Wadi sediments.

The prominence of sudden changes in the spacing of the magnetic contours over an appreciable distance, which trend mostly in the NNW-direction, suggests discontinuities in depth, possibly subsurface major faults. These faults caused left-lateral displacements, for the ENE-trending anomalies.

### 4.2.2. Regional-Residual Separation

The isolation of magnetic anomalies was carried out for the total magnetic intensity map depending on the results of energy spectrum analysis using a Geosoft Package (Geosoft Inc., 1995). The method was applied to the total magnetic data to obtain the average depth to the responsible subsurface geological sources as well as the differential magnetic response of each source ensemble that lie at a certain depth (Fig. 7). This operation resulted in the construction of two maps namely; the regional magnetic anomaly map (Fig. 8) at a depth of interface reaching 160 m and the residual magnetic anomaly map (Fig. 9) at a depth of interface reaching 43 m.

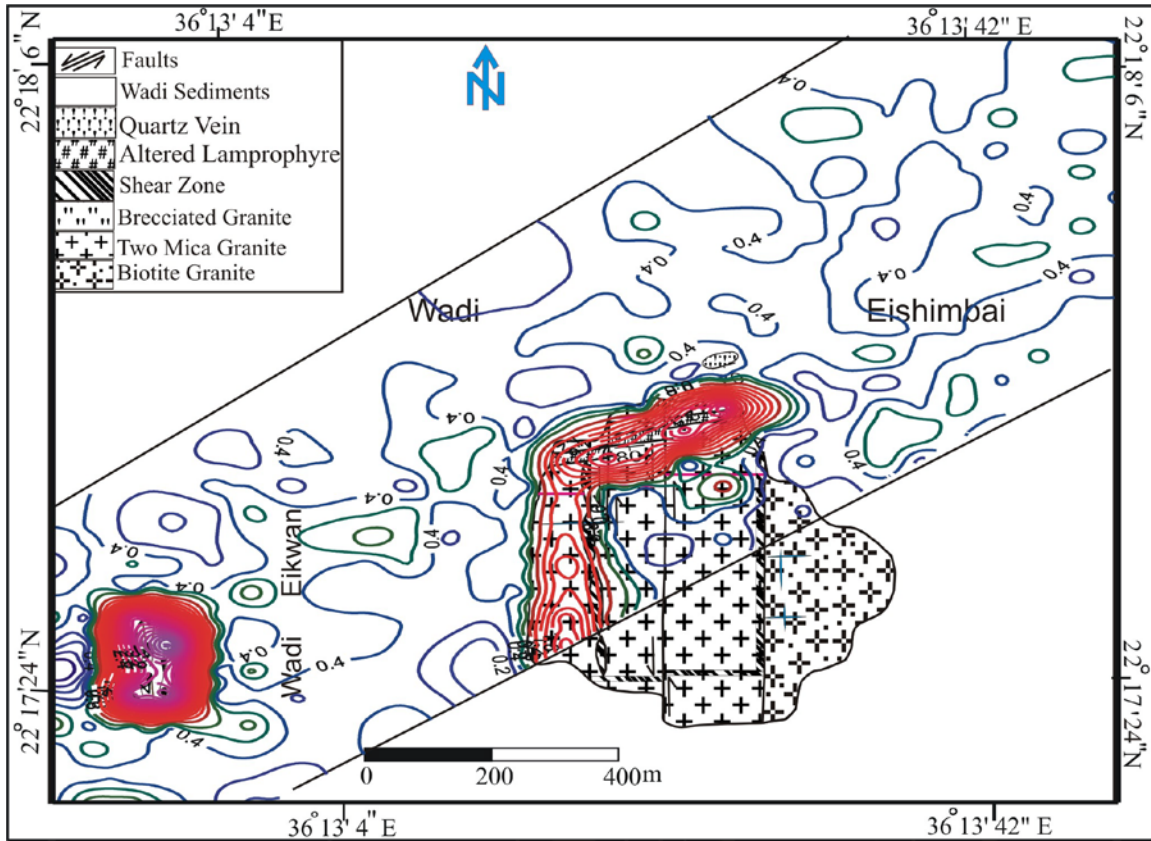


Fig. (5): eU/eTh ratio contour map of Wadi Eishimbai area, Southern Eastern Desert, Egypt.

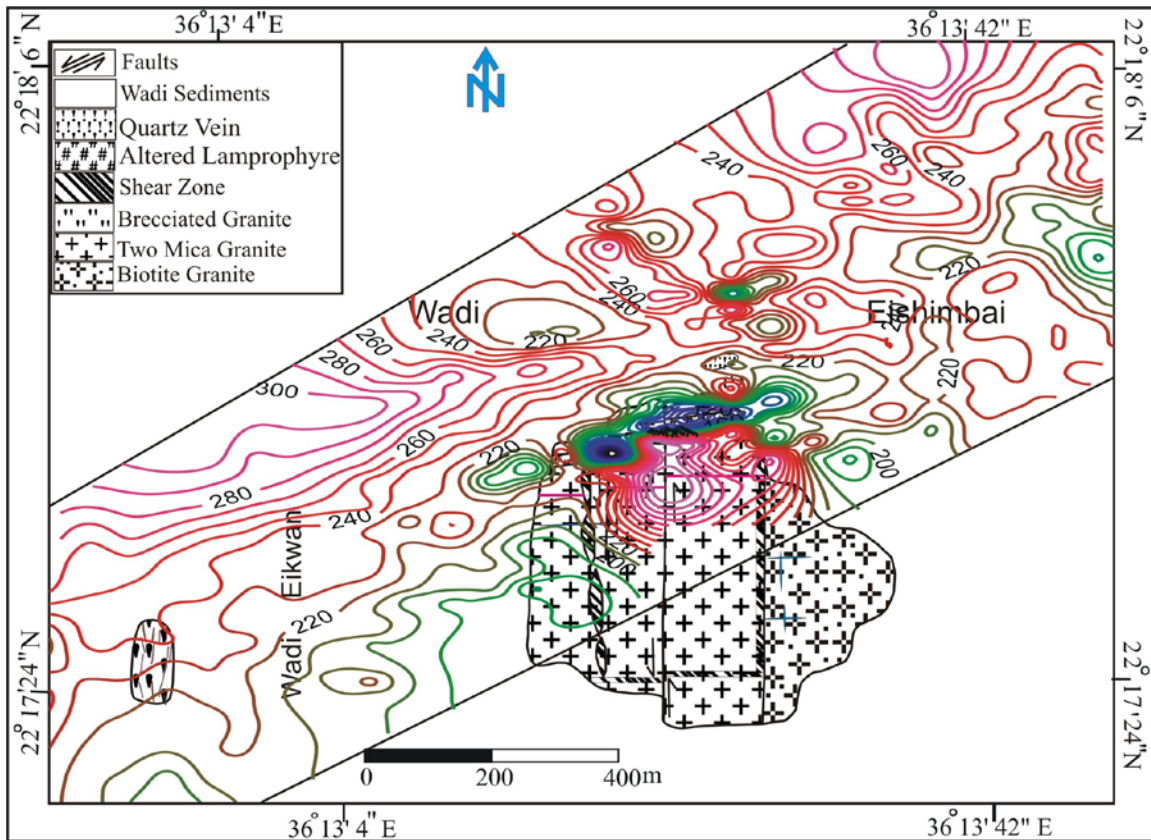


Fig. (6): Total magnetic field intensity (nT) contour map, with geologic background for Wadi Eishimbai area, Southern Eastern Desert, Egypt.

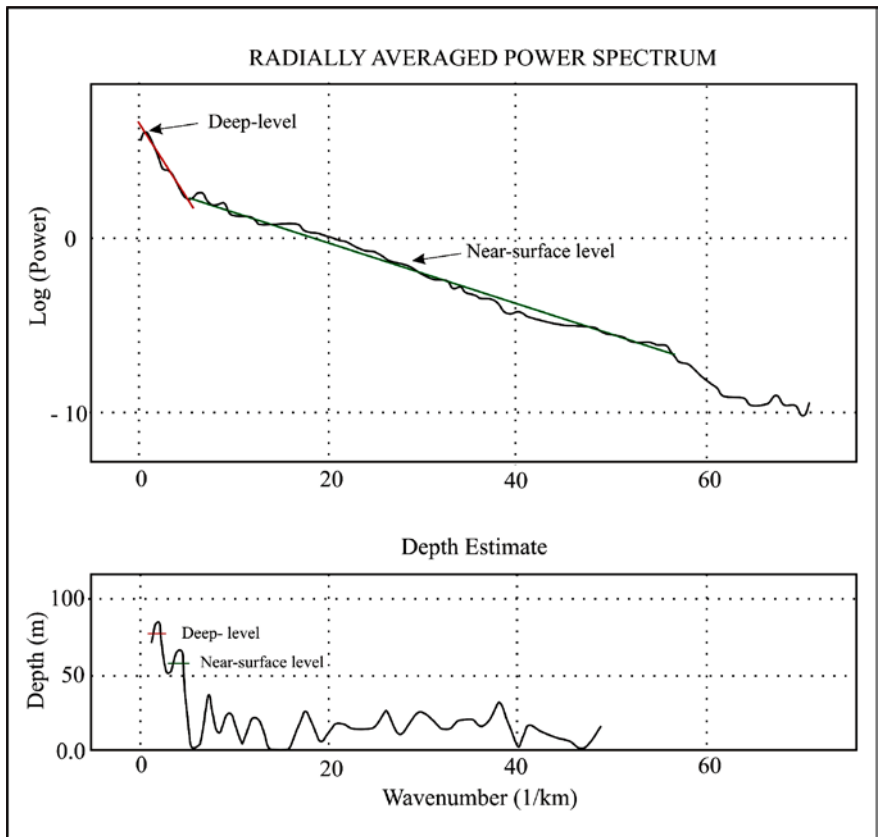


Fig. (7): Power spectrum showing the depth of deep-seated and near-surface magnetic sources for Wadi Eishimbai area, Southern Eastern Desert, Egypt.

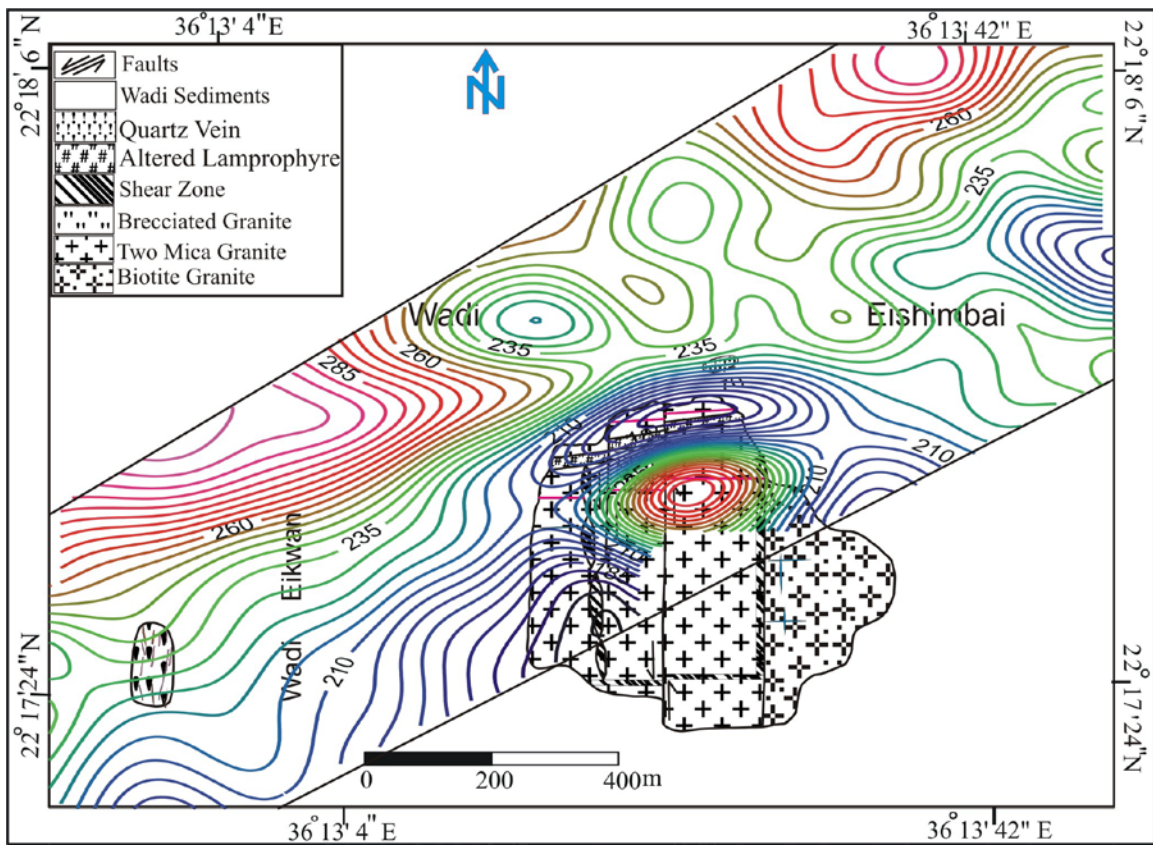


Fig. (8): Regional magnetic-anomaly contour map, with geologic background for Wadi Eishimbai area, Southern Eastern Desert, Egypt.



### 4.2.3. Regional Magnetic Anomaly Map

The regional contours are generally elongated in the ENE- and NW- directions (Fig. 8). The ENE-trending anomaly is superposed on a much broader, roughly oval-shaped magnetic high that extends away from the exposed Sela shear zone. The effect of the shear zone continues to about 300m to the west and then disappears. This may be due to a major graben with a width of about 300m. This graben is formed by two major normal faults trending in the NW-SE direction. To the west of this graben, there is a high oval-shaped anomaly, associated with the outcropping ENE-trending lamprophyre.

Strong positive magnetic anomalies located at the northern and northwestern parts of the study area coinciding with Wadi sediments also exist. These anomalies are due to the buried basic rocks, over which the granites are thrust. These anomalies are missed for about 400m, due to the effect of the major graben. The ENE- trending negative anomaly, elongated along the northern contact between the granitic body and Wadi sediments, becomes boarder than on the total magnetic field intensity map. It still extends in Wadi sediments along the western direction. This is due to the deep causative source.

### 4.2.4. Residual Magnetic Anomaly Map

A narrow zone embracing the surface projections of the lamprophyre falls along the axis of a high magnetic anomaly extending in the ENE-WSW direction in the study area (Fig. 9).

The absence of any magnetic expression in the northern and northwestern parts of the study area may be explained by the extension of magnetic deep-source or non-magnetic source bodies near the surface. The linearity and continuity of two anomalies of a NNW-trend suggest the presence of a parallel system of left-lateral strike-slip faults. The extension of the shear zone anomaly to the west becomes limited for only about 100 m to the west. This indicates that there is a western major graben and hence has not a shallow effect. Besides, the northern low-intensity magnetic anomaly disappears, to the west, due to the high effect thickness of the sediments. The outcropped lamprophyre at the west is characterized by a broad high-intensity magnetic anomaly, elongated in the ENE- direction.

### 4.2.5. Analytic Signal Magnetic Map

Nabighian (1972) introduced the analytic signal to calculate the dip and depth of 2D magnetic sources. Bastani and Pedersen (2001) used the analytic signal of the total magnetic field anomaly along a profile to estimate the dip, depth, width and strike of the dikes. Linping and Zhi-ning (1998) and Salem et al. (2002) showed that the maximum value of analytic signal from the total-field magnetic anomaly for a dipolar source is not always located directly over source. The analytic signal of the magnetic field is used to determine automatically the source parameters of dike-like structures. The Sela shear zone generates a conspicuous oval-shaped analytic signal of the total magnetic field intensity.

The analytic signal contour map (Fig. 10) shows that there is any response for the dike-shaped anomaly

for about 600 m on the Wadi sediments on the western side of the main shear zone. After that distance, an elongated high anomaly is associated with the outcropped lamprophyre, trending in an ENE- direction, for about 300m.

The lack of response of the anomaly, located at the northwestern margin of the study area, may be related to the shape of the causative body which may not be dike-like. The northern contact between the granitic body and Wadi sediments coincides with a prominent elongated high magnetic anomaly. This agreement with the total magnetic field intensity map suggests a buried shear zone or a major fault that extends parallel to the main shear zone in the ENE- direction.

## 5. VERY LOW FREQUENCY ELECTROMAGNETIC (VLF-EM) SURVEY

Because of the easy operation of the instrument, high speed of field survey, and low operation cost, this method is very suitable for rapid preliminary surveys and has been widely used in many geophysical studies since the 1960s (Bernard and Valla, 1991; Benson et al., 1997; Sharma and Baranwal, 2005). The VLF represents a valuable help to geological mapping. This method is a reconnaissance electromagnetic geophysical tool for mapping near-surface structures (Oskooi, 2004) using relatively simple instruments. It has been used successfully to investigate faults all over the world; examples include Nojima Fault and Ogura Fault (Yamaguchi et al., 2001), non-mineralized shallow fault zones (Jeng et al., 2004), groundwater-bearing zones (Sharma and Baranwal, 2005).

### 5.1. VLF-EM Field Procedure

The utilized instrument was the Scintrex VLF (ENVI VLF), Tronto, Canada, using two orthogonal VLF transmitters of frequencies  $F_1=17.1$  kHz, and  $F_2 = 28.5$  kHz. For tilt angle measurements, magnetic field coupling with the fracture zone is important. Therefore, the VLF-transmitter should be located along the strike of the target. The mid- frequencies ( $F = 28.5$  kHz) were parallel to the E-W trend of the sheared lamprophyre, whereas the low frequency ( $F = 17.1$  kHz) is perpendicular to it.

### 5.2. Results and Interpretation of VLF-EM Survey

The proposed scheme provided reliable conductivity- thickness and depth estimates for shear zone conductors provided that:

- (1) The conductor is nearly vertical and has large strike-length.
- (2) The host medium is homogeneous.
- (3) The survey lines are perpendicular to the strike of the conductor and to the VLF station.
- (4) The used survey frequencies are suitable and close to 17 kHz.

For interpretation, it is arguably better to use both the raw and filtered data. The effect of filtering the data was represented by two maps (Figs. 11 & 12).

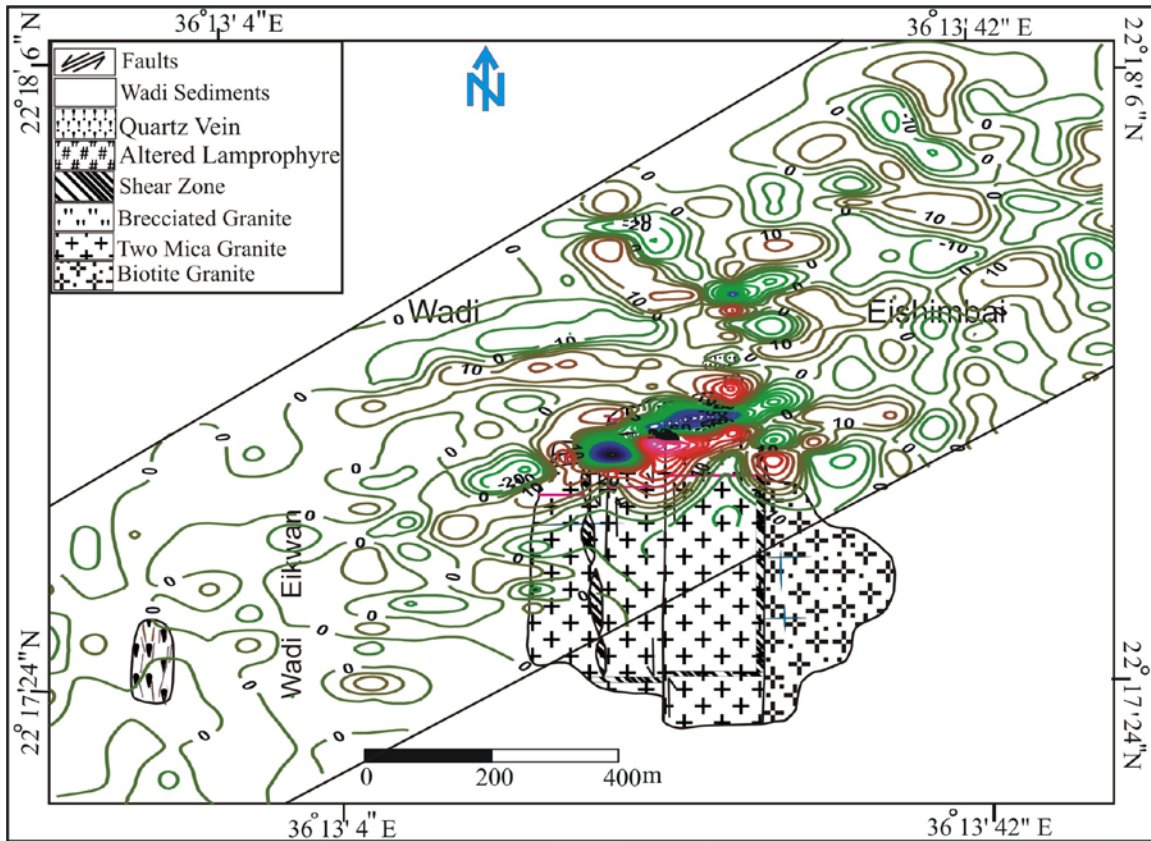


**Fig. (9): Residual magnetic-anomaly contour map, with geologic background for Wadi Eishimbai area, Southern Eastern Desert, Egypt.**

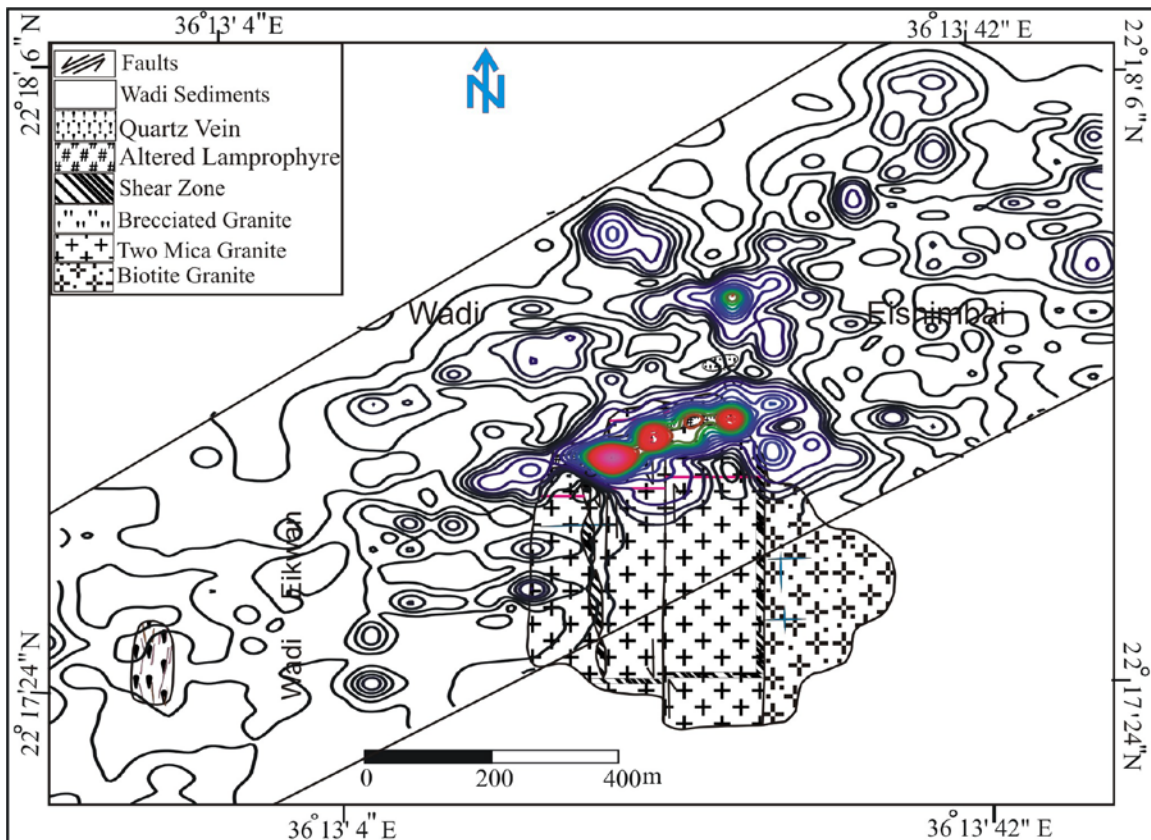


**Fig. (10): Analytical Signals of the total magnetic field contour map, with geologic background for Wadi Eishimbai area, South Eastern Desert, Egypt.**

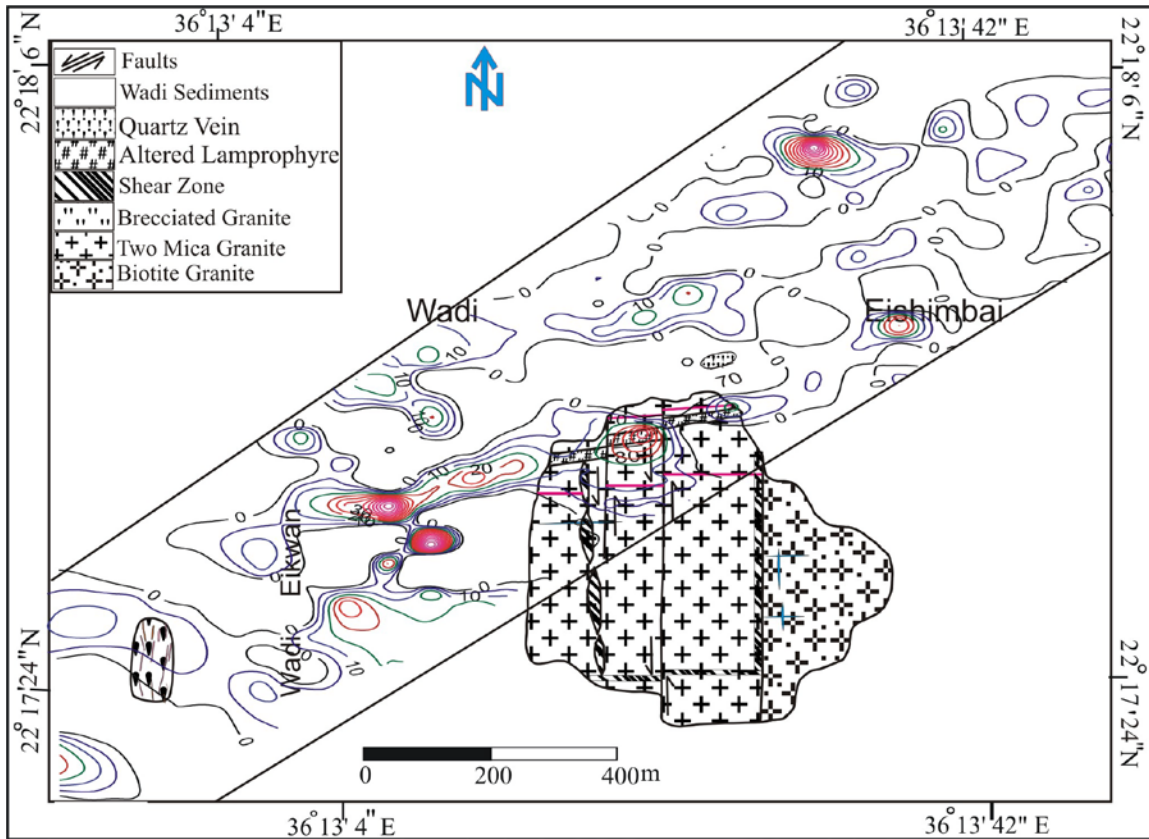


Fig. (11): VLF-EM Fraser filtered data (F=17.1 kHz) contour map, with geologic background for Wadi Eishimbai area, Southern Eastern Desert, Egypt.

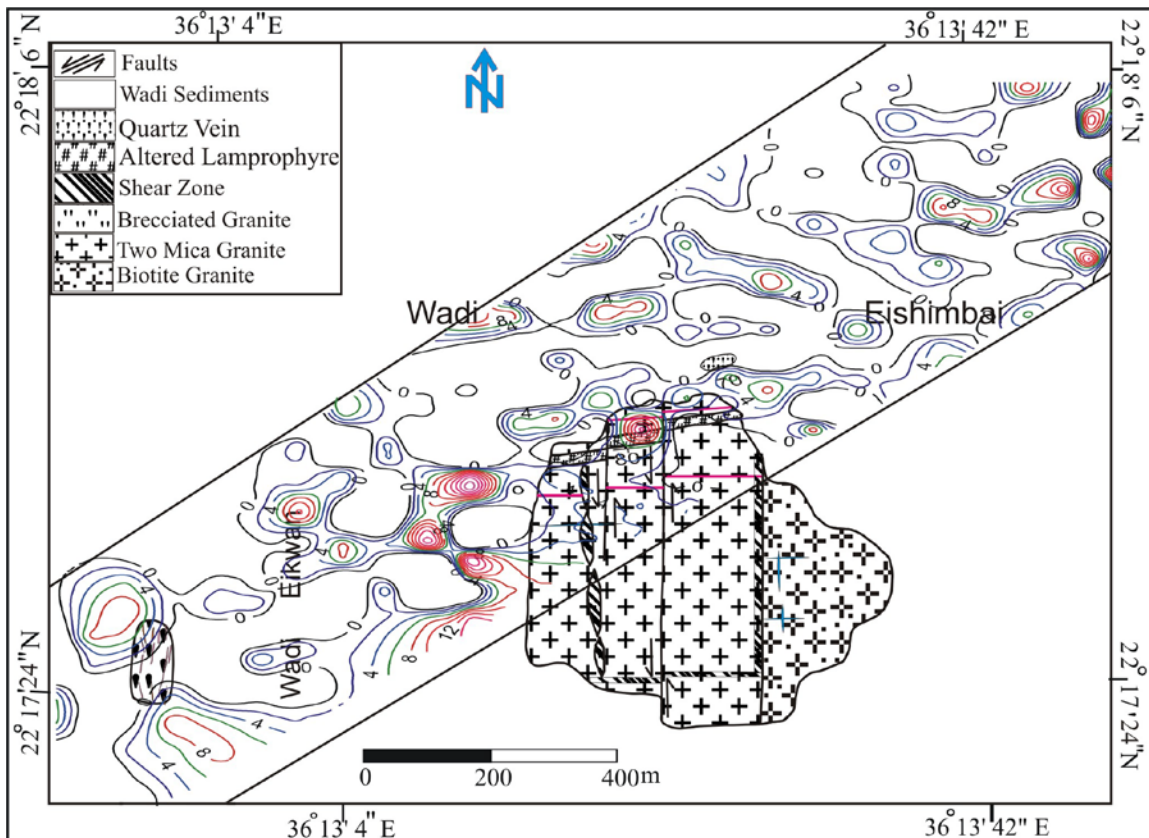


Fig. (12): VLF-EM Fraser filtered data (F=28.5 kHz) contour map, with geologic background for Wadi Eishimbai area, Southern Eastern Desert, Egypt.



### 5.2.1. Fraser Filtered VLF-EM Maps

The two used frequencies (17.1 and 28.5 kHz) displayed a remarkable agreement, in locating the shear zone conductors. The two filtered contour maps at the two frequencies 17.1 and 28.5 kHz (Figs. 11 & 12) showed that the shear zone is located within a strong conductive zone and outlined by the value 10. Meanwhile, the granitic rocks are associated with relatively weak conductivity zones that generally follow the NW- and E-W trending faults. However, larger scale apparent conductivity maps clearly display distinctive anomalies over Sela shear zone. These strong conductivity anomalies have great amplitudes, indicating an obvious exploration target. This is demonstrated particularly well in the central parts of the study area, where the sheared lamprophyre possesses high conductivities and predominates. The northern contact, showing a positive peak, is seen to have a shallow ascent, elongated in the ENE trend, due to conductive materials.

This suggests that the contact is structurally controlled. The separated parts of the positive anomalies associated with the shear zone and their displacements to the northeast are due to the parallel system of NNW-trending left-lateral strike-slip faults. The negative anomaly, located on the northeastern side of the study area, possesses a steep descent, indicating granitic resistive material. Consequently, close correlations were observed between the positive VLF anomalies and the

existing shear zone, which extends along the east-northeast trend. Meanwhile, pronounced negative VLF anomalies were recorded over the granite to the north and the south of the shear zone.

On the western side of the main shear zone, no trace for its continuity is observed for about 500m. However, the magnetic maps (Figs. 11 & 12) reflect an extension for the shear zone to about 300m to the west. This reflects that the shear zone, at that location, is downthrown or down faulted deep and show no shallow ascent. There are four concentric isolated high conductive anomalies, separated by distances ranging from 100 to 400m. Another high conductive anomaly is shown and elongated for about 250m along the ENE-direction. These anomalies are associated with the extension of the shear zone to the west, and affected by the NNW-trending strike slip faults. Moreover, these anomalies, except that anomaly which is associated with the outcropping lamprophyre, do not coincide with magnetic anomalies. These anomalies may correlate with the extension of the shearing zone that is rich in conductive materials.

## 6. STRUCTURAL INTERPRETATION

The ENE-trending shear zone is intersected by a NNW-trending left-lateral strike slip fault system, as shown on the interpreted structural lineament map, as deduced from the magnetic and conductivity data (Fig. 13).

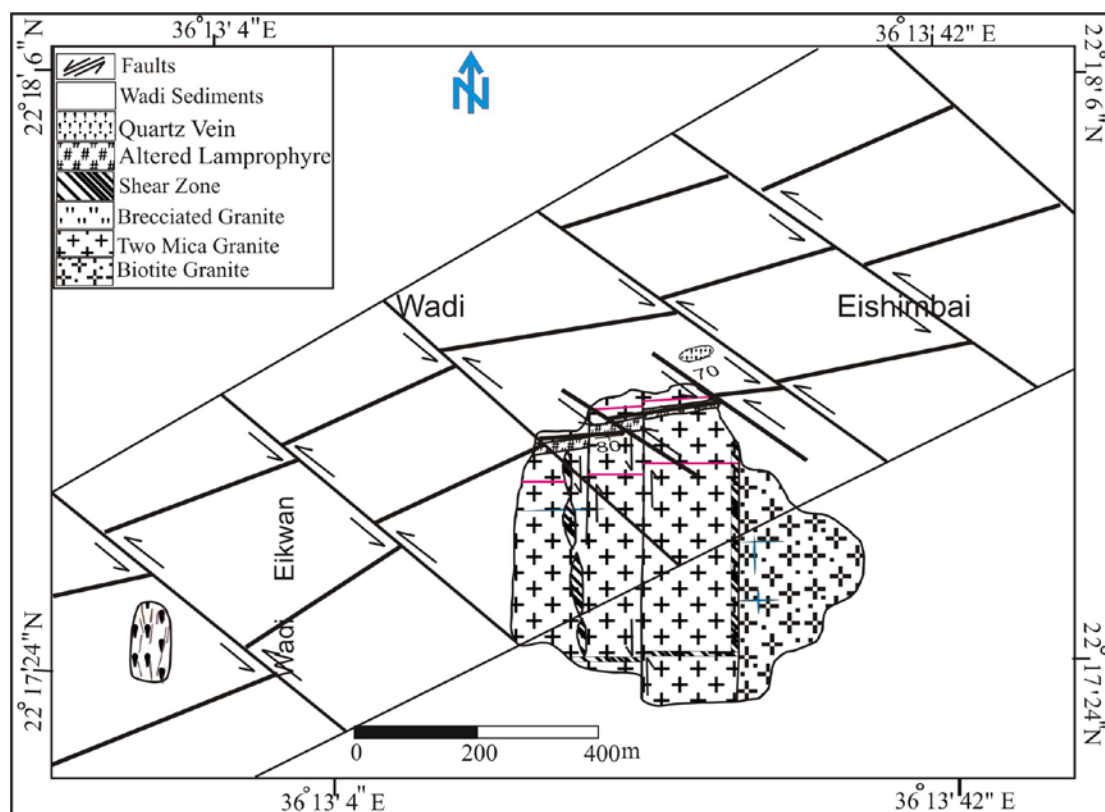


Fig. (13): Interpreted structural lineament map, as deduced from magnetic and VLF-EM maps, with geologic background for Wadi Eishimbai area, South Eastern Desert, Egypt.



Most of the NNW- trending faults cause sudden changes in the contour spacing over an appreciable distances, which suggest discontinuities in depth, due to their left-lateral strike slip displacements. The ENE-trending, interpreted group of faults, represents the main trend of the shear zone, through which hydrothermal solutions were flowing causing the highly alteration and uranium mineralization. This trend denotes an important structural phase, that controls another set of microgranite, quartz, lamprophyre and brecciated granite dikes in the study area. These dikes are highly radioactive and some of them are associated with uranium mineralization. Therefore, it is worthy to mention that the complicated lithologic and structural history of the study area represent a promising criteria for uranium fertility. Another detected major fault or shear zone, trending parallel to the main shear zone, mainly lies at the northern part of the studied area. This fault is of a deep-source and is dissected and displaced by the NNW- trending faults.

## CONCLUSIONS

The ENE-WSW lamprophyre dikes dissecting the north granites are massive, fine-grained black groundmass, with alkali feldspar phenocrysts. They have higher U-content, many times greater than the granite. These zones were the channel for the fluids, involved in all the uranium concentration steps, which may lead to the formation of U-ore bodies in the area. The eTh distribution discriminated the eastern parts of biotite granites, ranging from 8 to 30 ppm, than the two-mica granite in the western part of the studied area that possesses values 10 to > 80 ppm eTh. The brecciated granite in this area is leucocratic and mainly composed of quartz, feldspars and muscovite/biotite mica. Some intensive alteration features, such as hematitization and illitization are recorded where a set of parallel N-S faults are present. The process of uranium mobilization is very important as such altered rocks were subjected to mineralized bearing solutions.

The eU/eTh ratio distribution indicates that the brecciated granite shows promising anomalies and their radiometric signatures are characterized by high anomaly elongated in the N-S direction in southwestern part of the study area. Meanwhile, the N-S shear zone shows also high content of eU over eTh levels, trending in the NNW-direction. These vein types mineralization possess higher U-content many times greater than the granite, leading to an increase in the U-potentiality, which might lead to U-mobilization and possibly local uranium entrapment in the study area.

According to the strong contrast between the magnetic susceptibilities of the sheared basic lamprophyre, and the surrounding granites, magnetic survey succeeded in determining the expected subsurface extension of the shear zone and its contacts with the surrounding rocks. On the western side of the main shear zone, there is no VLF-trace for its continuity

is observed for about 500m. However, the magnetic maps reflect an extension for the shear zone to about 300m to the west. This reflects that the shear zone, at that location, is downthrown or down faulted deep and has not shallow ascent.

Most of the NNW-trending faults cause left-lateral strike slip displacements and associated with U-enrichment. The ENE-trending, interpreted as the old group of faults, represents the main trend of the shear zone, through which hydrothermal solutions were flown causing the highly alteration and uranium mineralization. The association of radioactivity, conductivity and magnetic anomalies in Wadi Eishimbai area can represent a sufficient indication to that target as one of the most promising uranium vein-type and a good trap for uranium-rich fluids or uranium ores. Accordingly, it will be promising for drilling to evaluate the expected uranium deposit associated with the shear zone. The locations of the suggested wells must be to the south of the shear zone, with direction of drilling towards north to cross the target that dips to the south.

## REFERENCES

- Abdel Fattah, T. A., 2007.** Application of well log tools and organic geochemistry in source rock identification, southern Gulf of Suez, Egypt (abs.). GSA Denver Annual Meeting (28–31 October 2007).
- Alsharhan, A.S., 2003.** Petroleum geology and potential hydrocarbon plays in the Gulf of Suez rift basin, Egypt. AAPG Bull., 87 (1), 143–180.
- Bosworth, W., Crerello, P., Winn Jr, R.D., and Steinmetz, J., 1998.** Structure, sedimentation, and basin dynamics during rifting of the Gulf of Suez. In (Eds.), Purser, B.H. and Bosence, D.W.J. Sedimentation and Tectonics of Rift Basins: Red Sea – Gulf of Aden, 78-96.
- Egyptian General Petroleum Corporation, EGPC, 1996.** Gulf of Suez oil fields (A comprehensive overview), 736 p.
- El-Shahat, W., Villinski, J. C., and El-Bakry, G., 2009.** Hydrocarbon potentiality, burial history and thermal evolution for some source rocks in October oilfield, northern Gulf of Suez, Egypt. Journal of Petroleum Science and Engineering, 68, 245–267.
- El Sharawy, M.S., 2006.** Seismic and well log data as an aid for evaluating oil and gas reservoirs in the southern part of the Gulf of Suez, Egypt. PhD dissertation, Mansoura University, Egypt, 265 p.
- Espitalie, J., Madec, M., Tissot, J., Menning, J., Leplat, P., 1977.** Source rock characterization method for petroleum exploration. Proc., 9<sup>th</sup> Annual Offshore Technology Conf., 3, 439–448.

- Hunt, J.M., 1995.** Petroleum Geochemistry and Geology. W.H. Freeman and Company, New York. 743 pp.
- Hood, A., Gutjahr, C.C. M., and Heacock, R.L., 1975.** Organic metamorphism and the generation of petroleum. AAPG Bull., 59 ( 6), 986-996.
- Khalil, B. A., 1993.** Reservoir evaluation in the southern part of the Gulf of Suez and its structural relationship. Ph.D. dissertation, Ain Shams University, 247 p.
- Lopatin, N.V., 1971.** Temperature and geologic time as factors in qualification (in Russian): Akad. Nauk. SSSR Izv. Ser Gel., 3, 95-106.
- Mallick, R.K., and Raju, S.V., 1995.** Thermal maturity evaluation by sonic log and seismic velocity analysis in parts of Upper Assam Basin, India. Org. Geochem., 23 (10), 871-879.
- Meyer, B.L., and Nederlof, M.H., 1984.** Identification of source rocks on wireline logs by density/resistivity and sonic transit time/ resistivity cross plots. AAPG Bull. 68, 121– 129.
- Myers, K.J., and Jenkyns, K.F., 1992.** Determining total organic carbon content from well logs: an intercomparison of GST data and a new density log method. Geological applications of wireline logs II. In (Eds), Hurst, A., Griffiths, C.M., Worthington, P.F., Geol. Soc. London, Spec. Publ., 65, 369-376.
- Passey, O.R., Moretti, F.U., and Stroud, J.D., 1990.** A practical model for organic richness from porosity and resistivity logs. AAPG Bull. 74, 1777–1794.
- Peters, K.E., 1986.** Guidelines for evaluating petroleum source rock using programmed pyrolysis. AAPG Bull. 70, 318– 329.
- Robertson Research International (RRI), 1986.** The Gulf of Suez area, Egypt: stratigraphy, petroleum geochemistry, petroleum geology, six volumes Robertson Group, Leandudno.
- Robertson Research International (RRI), 1984.** Results of "rock-eval" pyrolysis analyses of cuttings and core samples from haltenbanken well: 6507/12-1, Report no. 5406P/D, 24 p.
- Robertson Research (US) Inc., 1983.** Geochemical analysis of north Aleutian Shelf, Cost no. 1 well, Alaska, Report no. 823/135, 318 p.
- Said, R., 1990.** Cretaceous paleogeographic maps. in R. Said: Geology of Egypt, 1990, 439-449.
- Salah, M.G., and Alsharhan, A.S., 1998.** The Precambrian basement: A major reservoir in the rifted basin, Gulf of Suez. Journal of Petroleum Science and Engineering 19, 201–222.
- Schmoker, J.W., 1981.** Determination of organic-matter content of Appalachian Devonian shales from gamma-ray logs. AAPG Bull. 65, 2165–2174.
- Schmoker, J.W., 1979.** Determination of organic content of Appalachian Devonian shales from formation - density logs. AAPG Bull. 63, 1504-1509.
- Schmoker, J.W., and Hester, T.C., 1983.** Organic carbon in Bakken Formation, United States portion of Williston Basin. AAPG Bull. 67, 2165–2174.
- Staplin, F.L., 1969.** Sedimentary organic matter, organic metamorphism, and oil and gas occurrence. Canadian Petroleum Geology Bull., 17, 47-66.
- Tissot, B.P, Pelet, R., and Ungerer, P., 1987.** Thermal history of sedimentary basins, maturation indices, and kinetics of oil and gas generation. AAPG Bull., 71 (12), 1445-1466.
- Tissot, B.P., and Welte, D.H., 1984.** Petroleum Formation and Occurrence. Springer-Verlag, New York, 966 p.
- Waples, D.W., 1980.** Time and temperature in petroleum formation: application of Lopatin's method to petroleum exploration. AAPG Bull., 64 (6) (June), 916-926.